DesignCon 2008

Exploration of Deterministic Jitter Distributions

Michael Steinberger, Signal Integrity Software, Inc.
msteinb@sisoft.com, 715-720-4112

Abstract

While Deterministic Jitter (DJ) is generally agreed to be peak limited, what is less clear is how rapidly its PDF decreases near that limit, especially when the DJ is due to crosstalk.

This paper addresses this and related questions by considering a class of responses which are similar to real system responses but are described by closed form equations. These responses can therefore be evaluated precisely at arbitrary times, allowing the tails of the jitter distribution to be explored in detail. The result is a clearer understanding of when the tails of a DJ PDF can resemble a Gaussian.

Author's Biography

Dr. Michael Steinberger is currently responsible for leading the development of SiSoft's serial link analysis products. He has over 29 years experience in the design and analysis of very high speed electronic circuits. Prior to joining SiSoft, Dr. Steinberger worked at Cray Inc., where he designed very high density interconnects and increased the data rate and path lengths to the state of the art. Mike holds a B.S. from the California Institute of Technology and a Ph.D. from the University of Southern California, and has been awarded 7 U.S. patents.

1.0 Motivation

It is generally accepted that for any linear, time-invariant digital channel with constant data rate and no impairments other than intersymbol interference, there exists a finite boundary to the inside of the eye diagram. Furthermore, the positive side of that finite boundary can be calculated by subtracting the absolute values of the intersymbol interference due to each symbol in the data stream from the pulse shape for a positive data bit (i.e., "one"), and the negative side of that boundary can be calculated using an analogous procedure for a negative data bit (i.e., "zero). This is, for example, the principle behind peak distortion analysis [1].

The existence of this finite boundary is also the principle behind the concept of deterministic jitter (DJ). Intersymbol interference is a deterministic process in the sense that it is determined directly by the data pattern; and the existence of a finite bound on the inside the eye leads to the observation that DJ is peak limited.

There remains, however, the question as to exactly how rapidly the calculation of the inner eye boundary converges. Will the calculation come within a few percent of the limit after a few symbols or will it take hundreds of symbols to obtain an accurate calculation of that limit?

Similarly, crosstalk from adjacent data signals is sometimes considered to be a form of DJ in the sense that these data signals can be controlled. Crosstalk is also sometimes considered to be a form of random jitter (RJ) in that the crosstalk coupling mechanism is so complex that the resulting amplitude or jitter PDF due to crosstalk is assumed to be Gaussian, and can therefore be combined with other Gaussian disturbances such as the effects of shot noise.

The question addressed in this paper is therefore how "sharp" the edges of an eye diagram are, either for a desired signal or a crosstalk signal. If only a few symbols are required to converge to an inner eye boundary, then the probability density function (PDF) of the jitter due to intersymbol interference will drop off quite rapidly near the maximum jitter, indicating a "sharp" eye; whereas if many symbols are required to approach the inner eye boundary, then the PDF of the jitter due to intersymbol interference will drop off much more slowly, indicating a "soft" eye.

The answer to this question has practical implications in that it defines a lower limit to the number of adjacent bits which must be included in a peak distortion analysis or a bit error rate estimate in order to achieve a desired level of precision.

It also has some practical implications for test equipment which separates DJ from RJ in that the general method for doing so is to fit a Gaussian curve to the tails of a measured jitter distribution and attribute those tails to RJ. Unless one knows how sharp the edges of a deterministic eye are, it is not immediately clear how much of the RJ measured in this way is due to black body radiation, shot noise, power supply noise, waiting time jitter, or intersymbol interference. Furthermore, with a better understanding of the sharpness of a

deterministic eye, it may be possible to estimate to how many standard deviations the Gaussian curve must be fit in order to reliably separate DJ from jitter due to truly random sources.

2.0 Approach

A rigorous approach to this question must separate the effects of numerical or model accuracy from effects which are fundamental to the phenomenon of intersymbol interference. The approach taken here therefore considers intersymbol interference from several perspectives.

The first calculation of intersymbol interference uses closed form pulse response equations for a widely known class of ideal, band limited spectral shapes which are said to possess Nyquist I symmetry [2], and therefore have zero intersymbol interference at the center of the eye. The most widely known of these shapes are called cosine rolloff channels [2]; however, there is another type of response which could be called "linear rolloff" which also has Nyquist I symmetry and more closely resembles the response of a broadband digital channel. Since the equations are closed form, the pulse response can be calculated for arbitrary times with a high degree of accuracy without any concerns about sampling interval or interpolation accuracy.

The second calculation of intersymbol interference is for an electrical transmission path described by realistic physical parameters and equalized with a very good equalization solution. It will be seen that the resulting pulse response closely resembles a linear rolloff pulse response. This should not be too surprising in that the transfer function of the transmission path decreases very rapidly with frequency, and the frequency response of both the finite impulse response (FIR) and rational transfer function components of the equalization solution rolls off for frequencies near and above the data rate as well, resulting in a spectral shape which is practically band limited. Furthermore, the equalization solution is designed to minimize intersymbol interference in the center of the eye, so the resulting frequency response comes close to achieving Nyquist I symmetry, just like the linear rolloff frequency responses.

3.0 Nyquist Pulse Shape Equations

In order to have zero intersymbol interference in the center of the eye, the Fourier transform $R(f)$ of a pulse shape $r(t)$ must have so-called Nyquist I symmetry. If the symbol period is T and the Fourier transform of the pulse shape is further constrained to be zero for all frequencies above $1/T$, then the frequency response at one half the data rate must be half of the frequency response at DC. That is,

$$R\left(\frac{1}{2T}\right)=\frac{1}{2}R(0)$$

Furthermore, the frequency response must exhibit odd symmetry about one half the data rate. That is,

$$R\left(\frac{1}{2T}-f\right)+R\left(\frac{1}{2T}+f\right)=R(0)$$

Traditionally, the most popular Nyquist symmetric pulse shapes have been pulse shapes for which the frequency response in the region around half the data rate is described by a raised cosine function. These are usually called cosine rolloff responses, and are widely used in digital radio systems because of their bandwidth efficiency. I did solve the equations for a cosine rolloff pulse shape and was able to check my results by reproducing the known characteristics of these responses; however, the resulting pulse shapes exhibited a ringing which took many symbol times to decay to a negligible value. These pulse shapes clearly were not a good representation for the pulse response of a high speed serial channel. While I did not pursue the question any further, it would be reasonable to suppose that the ringing is due to the rapid fall off of the frequency response around half the data rate.

There are, however, many other responses which exhibit Nyquist symmetry, including linear rolloff (trapezoidal) and truncated triangular. I chose the linear rolloff shapes because they are continuous and have relatively small slope at all frequencies.

The class of linear rolloff pulse responses is defined in the frequency domain by the equations

$$R(f)=r_0T \qquad 0\le|f|\le(1-b)\frac{1}{2T}$$

$$R(f)=r_0T\left(\frac{1+b}{2b}-\frac{T}{b}|f|\right) \qquad (1-b)\frac{1}{2T}<|f|\le(1+b)\frac{1}{2T}$$

$$R(f)=0 \qquad (1+b)\frac{1}{2T}<|f|$$

where the valid values for the rolloff factor b are between 1 and 0, and T is the bit period.

Taking the Fourier transform of this response,

$$r(t)=2r_0T\int_0^{(1-b)\frac{1}{2T}}\cos(2\pi ft)\,df$$

$$+2r_0T\frac{1+b}{2b}\int_{(1-b)\frac{1}{2T}}^{(1+b)\frac{1}{2T}}\cos(2\pi ft)\,df$$

$$-2r_0T\frac{T}{b}\int_{(1-b)\frac{1}{2T}}^{(1+b)\frac{1}{2T}}\cos(2\pi ft)\,f\,df$$

Evaluating the integrals,

$$
\begin{aligned}
r(t) = r_0 \frac{T}{\pi t}\sin\left((1-b)\frac{\pi t}{T}\right) \\
+ r_0 \frac{1+b}{b}\frac{T}{2\pi t}\left(\sin\left((1+b)\frac{\pi t}{T}\right) - \sin\left((1-b)\frac{\pi t}{T}\right)\right) \\
- \frac{2r_0}{b}\left(\frac{T}{2\pi t}\right)^2\left(\cos\left((1+b)\frac{\pi t}{T}\right) - \cos\left((1-b)\frac{\pi t}{T}\right)\right) \\
- \frac{2r_0}{b}\frac{T}{2\pi t}\left(\frac{1+b}{2}\sin\left((1+b)\frac{\pi t}{T}\right) - \frac{1-b}{2}\sin\left((1-b)\frac{\pi t}{T}\right)\right)
\end{aligned}
$$

This equation, then, describes in closed form the class of pulse shapes studied.

4.0 Comparison to a Practical Channel

The pulse response for an example of a practical channel 5 Gb/s channel was compared to the family of linear rolloff pulse responses. The model of the practical channel consists of a detailed model of a lossy transmission line followed by a receiver containing a peaking filter and DFE.

The model of the transmission path is realistic in the sense that the effects of both the variation of dielectric constant with frequency [3] and the internal impedance of the conductors [4] are included in the model. It is somewhat idealized, however, in that it does not include packages, vias, connectors, or termination mismatch. Thus, this model is reasonably realistic up to approximately 3 GHz, and increasingly optimistic for frequencies higher than 3 GHz. For a 5 Gb/s data rate, the electrical path is a 17dB loss path (i.e., 17dB loss at 2.5GHz), which is about in the middle of the typical range of practical electrical paths for systems currently in production.

The receiver model includes a linear peaking amplifier followed by clock recovery, a decision circuit model, and DFE. Both the clock recovery and DFE are fully adaptive, and the decision circuit model includes the effects of minimum latch overdrive. This model is described in more detail in a companion paper [5].

The details of the channel example are:

Electrical Path

Materials:	0.5 oz copper conductors and FR4 dielectric
Length:	1.25m
Conductor Dimensions:	$1.25\text{x}10^{-4}$ x $1.25\text{x}10^{-5}$m
Dielectric Loss Tangent:	0.02 (0.014 + 0.006 for conductor roughness)
Dielectric Constant:	4.2 @ 1GHz
Impedance:	50Ω
Loss:	17dB @ 2.5GHz

Peaking Filter:

Zeroes:	-490MHz
Poles:	-4GHz, -5GHz

DFE:

Taps (normalized to 1V):	-.019, .024, -.002, -.008

The magnitude of the frequency response for the practical channel is shown on a ***linear*** scale in Figure 1, along with the frequency response for a 60% linear rolloff pulse shape and a 100% linear rolloff pulse shape. The linear scale was chosen to match the way that Nyquist symmetry is defined. The 100% linear rolloff pulse shape was included to illustrate the available range of linear rolloff responses.

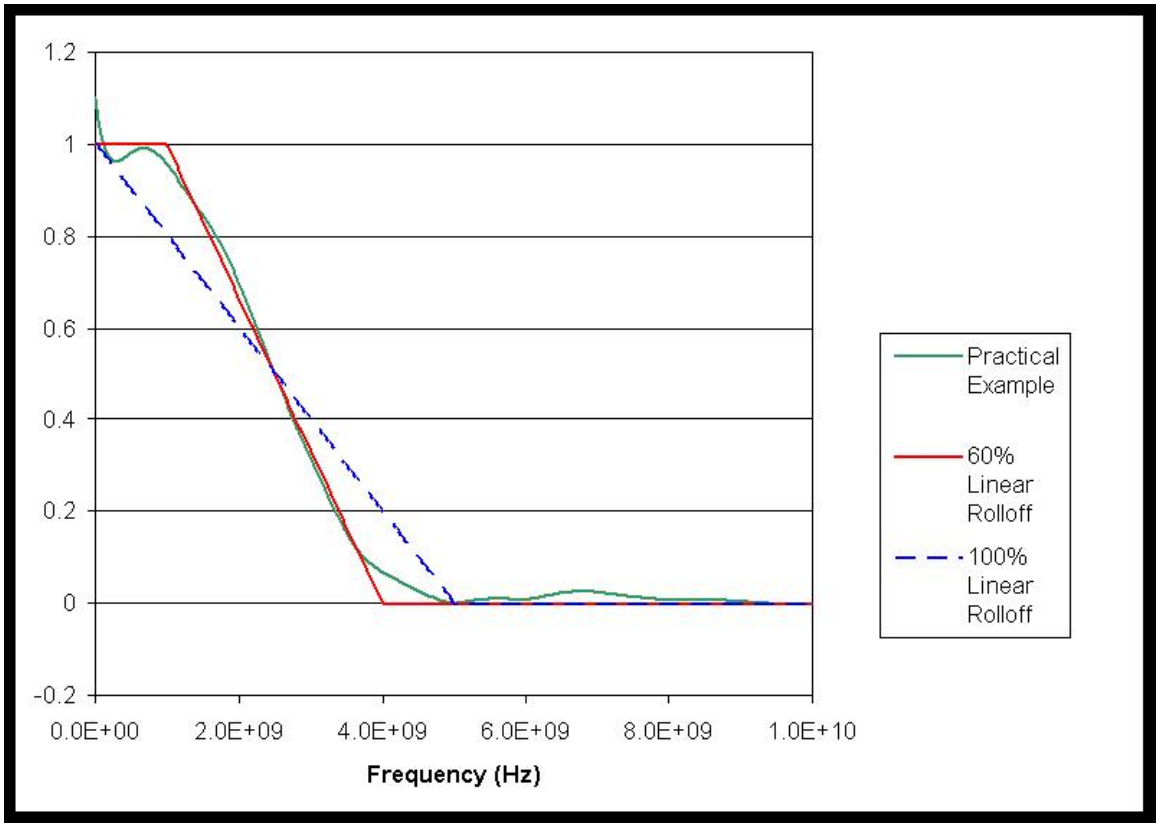

Figure 1: Frequency response comparison between practical channel and a 60% linear rolloff pulse shape

Note that the 60% linear rolloff response matches the practical channel response reasonably well over the range DC to 5GHz, and that the match is particularly good in the range 1.5GHz to 3.5GHz. Note also that although the practical channel response does have some energy in the range 6GHz to 8GHz, it's much less than the energy below 4GHz.

It would be possible to improve the match between ideal and practical responses by applying a windowing function such as a Gaussian to the ideal response, thus rounding off the sharp corners shown in Figure 1. Since the windowing function would be

multiplying in the time domain and convolving in the frequency domain, the result would be to truncate the linear rolloff response, thus making the edges of its eye somewhat harder because some of the contributors to any softening of the edges would be eliminated. This additional detail would, however, have detracted somewhat from the clarity of presentation without changing the conclusions significantly, and so I chose not to go to the extra effort.

Figure 2 compares the impulse response for the practical channel with the impulse response which would generate a 60% linear rolloff pulse response.

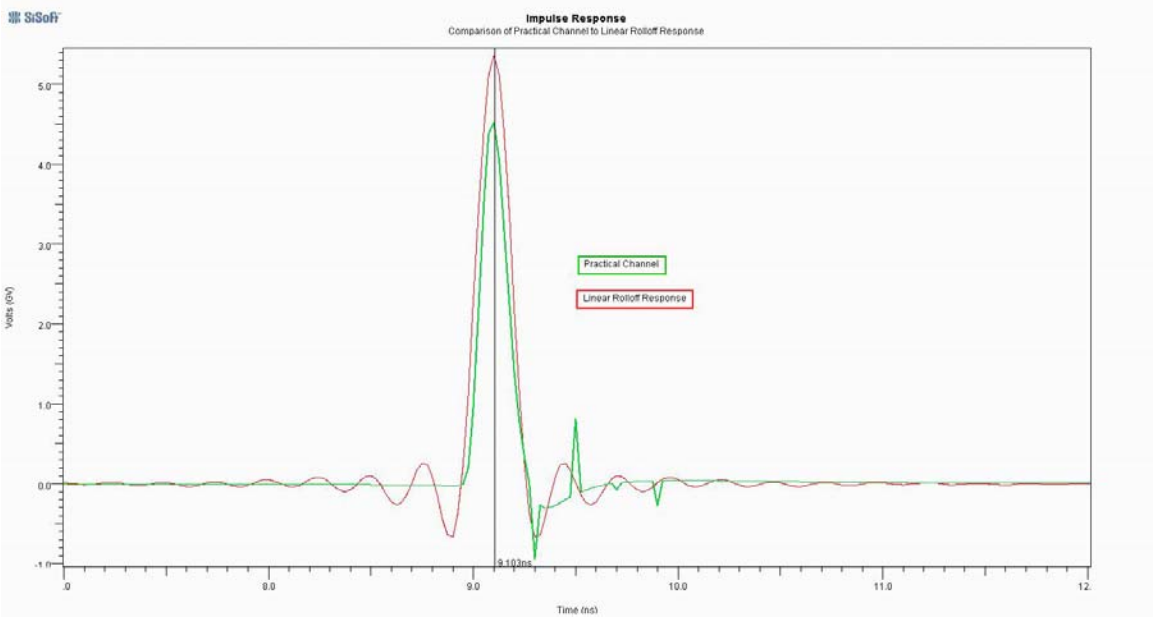

Figure 2: Impulse response comparison between practical channel and a 60% linear rolloff pulse shape

Note in Figure 2 that in the impulse response for the practical channel, the impulse response of the DFE has been included as a series of impulses following the main response.

In Figure 2, although the two impulse responses were shifted to line up in time, their vertical scales were purposely left different so that one impulse response did not obscure the other. While the main response and the first few post cursor ripples of the responses bear some similarity to each other, the linear rolloff impulse response has pre-cursor ripples whereas the practical channel impulse response does not. This illustrates that while the practical channel response is minimum phase (only left half plane zeroes- what many refer to as “causal”), the linear rolloff response is non-minimum phase (includes right half plane zeroes- what many refer to as “non-causal”).

Figure 3 shows an eye diagram obtained for the practical channel while Figure 4 is an eye diagram for the 60% linear rolloff response.

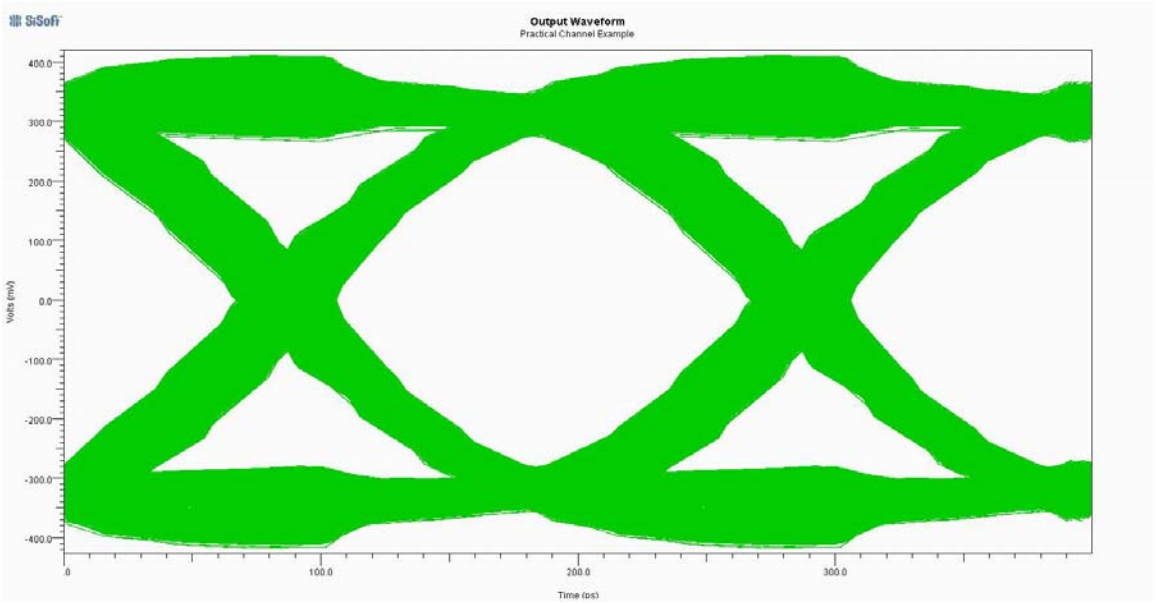

Figure 3: Eye diagram for a practical channel

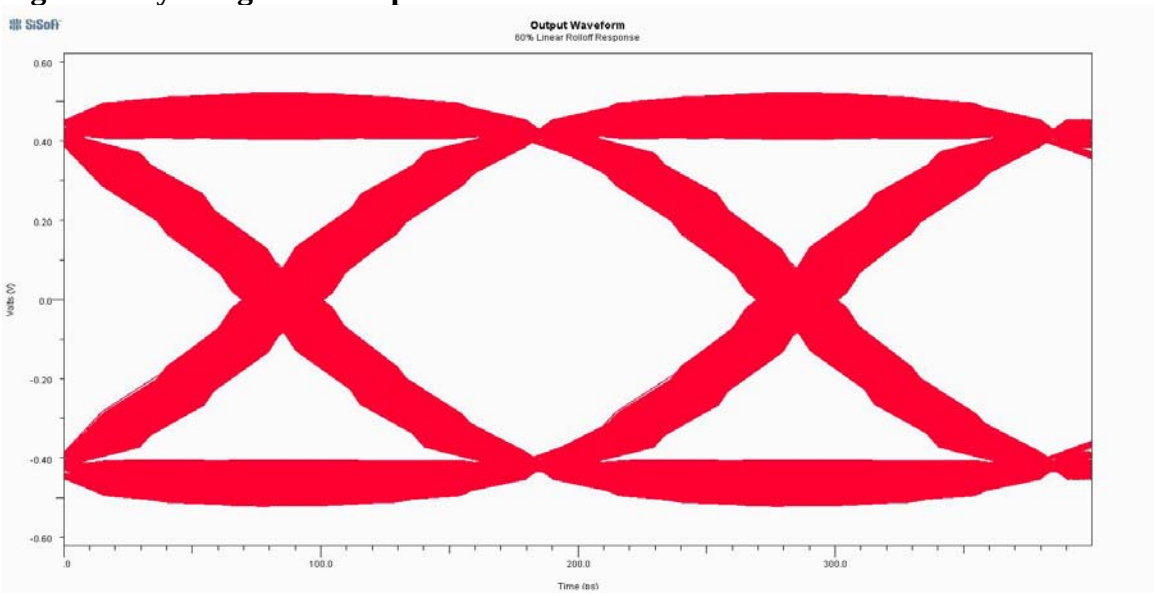

Figure 4: Eye diagram for a 60% linear rolloff response

While the 60% linear rolloff eye is somewhat cleaner, as one would expect, there is a considerable similarity between the two eyes.

One final observation about the comparison between linear rolloff responses and practical channels: There is no reason to expect that all practical channel responses will resemble a 60% linear rolloff response. Rather, the apparent linear rolloff may be different for different path losses and equalization solutions, and as yet there is no further data as to whether the similarity between channel response and linear rolloff response will tend to be better or worse than that demonstrated in this example.

5.0 Results

5.1 Peak Distortion Analysis

A spreadsheet exploration of the inner edge of the eye, as determined through peak distortion analysis, indicated that cosine rolloff responses, including 100% cosine rolloff, have essentially no guaranteed eye width, even though the guaranteed eye height in the exact center of the eye is 1.0 in all cases. Since cosine rolloff spectral shaping is used routinely with uniformly good results for microwave digital communications, this suggests that at least for this class of pulse shapes, peak distortion analysis is extremely conservative.

A similar exploration of linear rolloff responses generated much more promising results. Table 1 shows the results obtained when the calculation was based on an 800 bit message length.

Rolloff Factor	% Eye Width
1.0	88.61
0.9	90.62
0.8	91.84
0.7	92.08
0.6	88.6
0.5	81.22

Table 1: Eye width of linear rolloff responses as determined by peak distortion analysis

5.2 Jitter PDF

The PDF of the jitter caused by a 60% linear rolloff pulse response was computed using the closed form equation and convolution engine methods similar to those described in [6]. To minimize questions of numerical accuracy, the probability distribution function of the signal was represented as a histogram with a million bins, as opposed to the thousand bins recommended in [6]. For each time, the desired pulse was assumed to be a "one", and the probability distribution as a function of amplitude was integrated over all non-positive amplitudes. The result was then differentiated with respect to time to yield the PDF of the jitter.

Different numbers of bit positions were used in order to determine how many adjacent bit positions must be included in a calculation of intersymbol interference in order to obtain a specified level of accuracy. The results are plotted on a linear scale in Figure 5. Figure 5 also includes a fit to the curve that is built up as the sum of five Gaussian functions, and is therefore called a "Penta-Dirac" function. The standard deviation for the Gaussian functions is 0.0055UI.

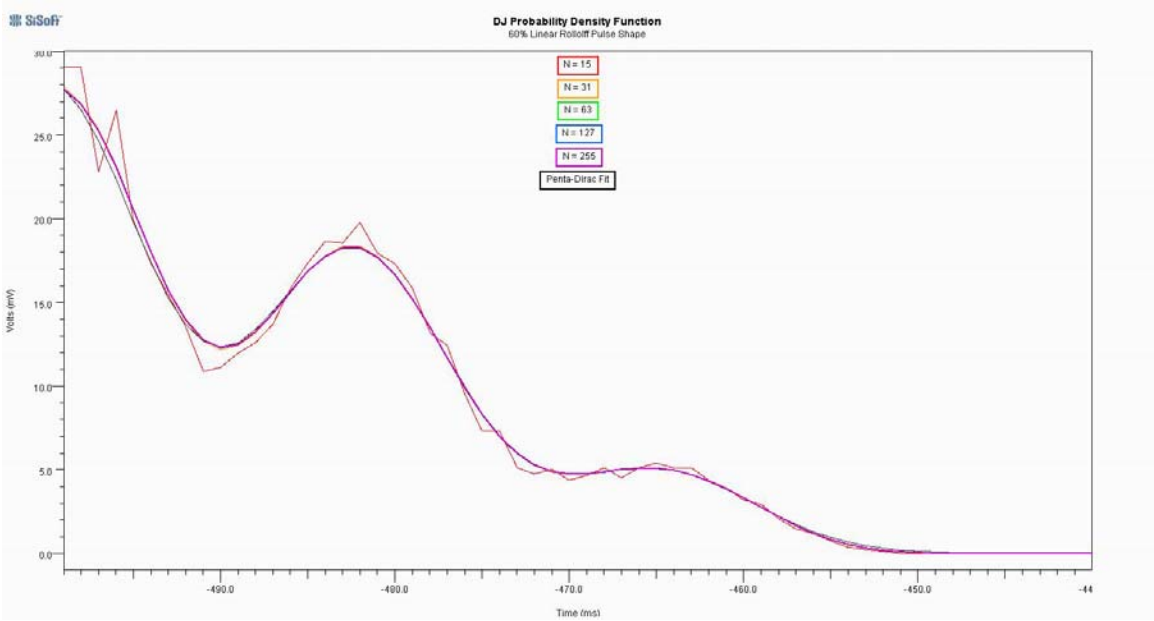

Figure 5: Deterministic Jitter PDF for 60% linear rolloff pulse response

From Figure 5, it would appear that with the exception of the message length of 15, all message lengths and the Penta-Dirac fit are in nearly perfect agreement.

Figure 6 plots the same data on a logarithmic scale, however, and it suggests different conclusions.

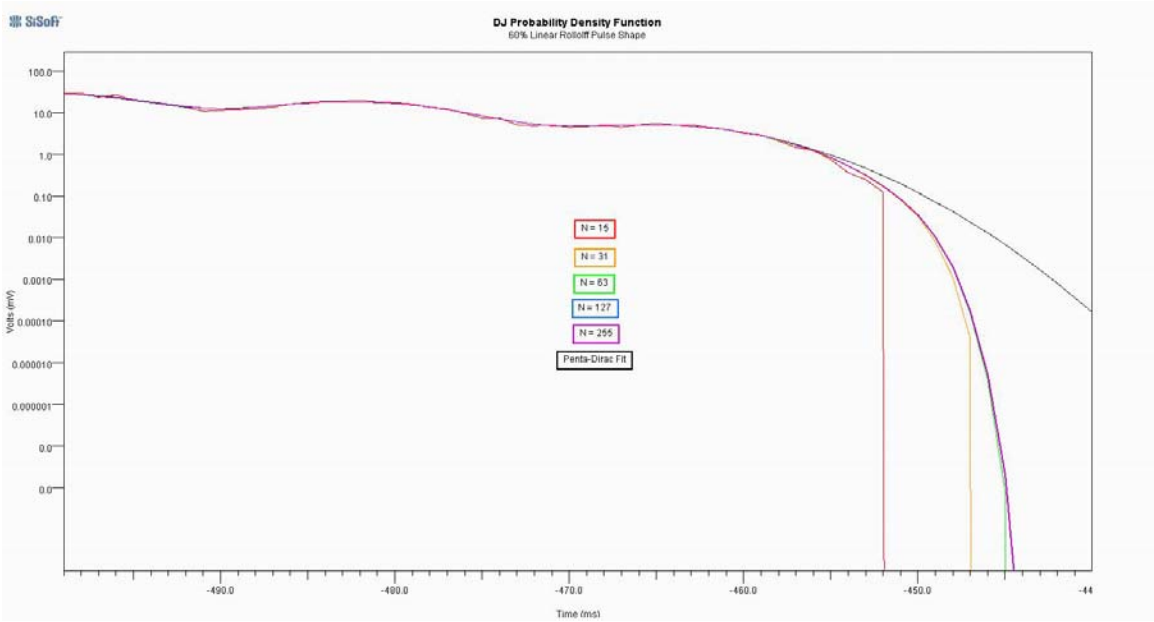

Figure 6: Log scale plot of Deterministic Jitter PDF for 60% linear rolloff pulse response

Figure 6 suggests the following conclusions:

1. The DJ PDF for this pulse response closely resembles a Gaussian distribution down to about 10% of peak density, but then falls off more rapidly than a Gaussian distribution.

2. Calculating the PDF from as few as 15 bit positions is not enough to obtain any reasonable level of accuracy.

3. Calculating the PDF from either 63 or 127 bit positions produces results with useful accuracy.

4. It does not seem necessary to calculate the PDF using more than 127 bit positions.

5. The tails of the PDF do extend to quite low probabilities before falling to identically zero.

5.3 Combining Jitter Components

Figures 5 and 6 also offer some insight into the general nature of the DJ distribution that can be applied to methods used for adding up jitter in a jitter-based performance budget. There are two methods for combining DJ that are generally used currently:

1. **Add the peak DJ Values.** This is a simple computation, which makes it easy to combine many components in a performance budget.

2. **Convolve the DJ PDFs together to get the combined PDF.** This is a much more rigorous method, but requires that one knows what the PDF of the DJ is, in addition to its peak value. The complexity of this method also makes it poorly suited to combining many components in a performance budget.

If the DJ were nearly uniformly distributed between its peak values or, better yet, distributed entirely at its peak values in a truly dual Dirac distribution, then the simplicity of method 1 above would make it an attractive choice, even if its repeated application would necessarily create an increasingly conservative result.

What Figures 5 and 6 suggest, however, is that DJ is far from being uniformly distributed. Instead, its PDF would appear to fall off quite substantially from a peak density in the middle of the distribution. In point of fact, the standard deviation for the DPF in Figure 5 is 0.0187UI whereas the peak deviation from mean is 0.057UI, or three times the standard deviation. Thus, any calculation based solely on the peak value of DJ is going to be excessively conservative.

Figure 7 contains the same data as Figure 5 except that the “Penta-Dirac” distribution has been replaced by a single Gaussian distribution whose standard deviation is the same as that for the actual DJ distribution.

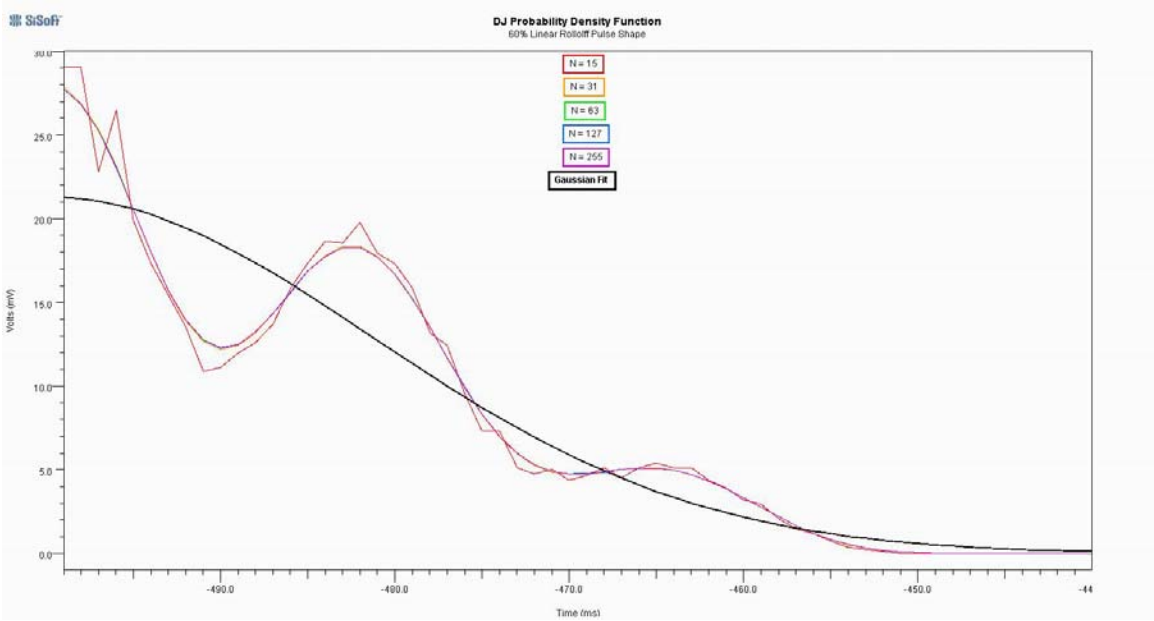

Figure 7: DJ Distribution with Gaussian fit

While the single Gaussian function does not fit the details of the distribution at all well, it does more or less fit the general shape. This suggests a method for combining DJ which is a compromise between methods 1 and 2 above:

1. Characterize a DJ distribution by its standard deviation and its peak deviation.
2. When combining two DJ components, take the rms combination of their standard deviations and add their peak deviation together to get a new standard deviation and peak deviation.
3. When using the individual or combined DJ in a performance calculation, estimate the PDF of the DJ as a Gaussian with the same standard deviation as the DJ, but then truncate that Gaussian at a value equal to the peak deviation of the DJ.

This method is almost as simple as method 1 above, and should yield reasonable accuracy for the amount of effort invested.

As an example, consider the case of compounding two instances of the DJ distribution shown in Figure 7. Following the steps outlines above,

1. The DJ distribution has a mean of -0.5 UI, a standard deviation of 0.0187 UI and a peak deviation of 0.057 UI.
2. If two instances of this distribution are compounded together, then the result will have a mean of -0.5 UI, a standard deviation of the square root of two times 0.0187, or 0.0264 UI, and a peak deviation of two times 0.057, or 0.114 UI.
3. Figure 8 shows the convolution of the PDF in Figure 7 with itself, along with the truncated Gaussian distribution with the same mean, standard deviation, and peak deviation.

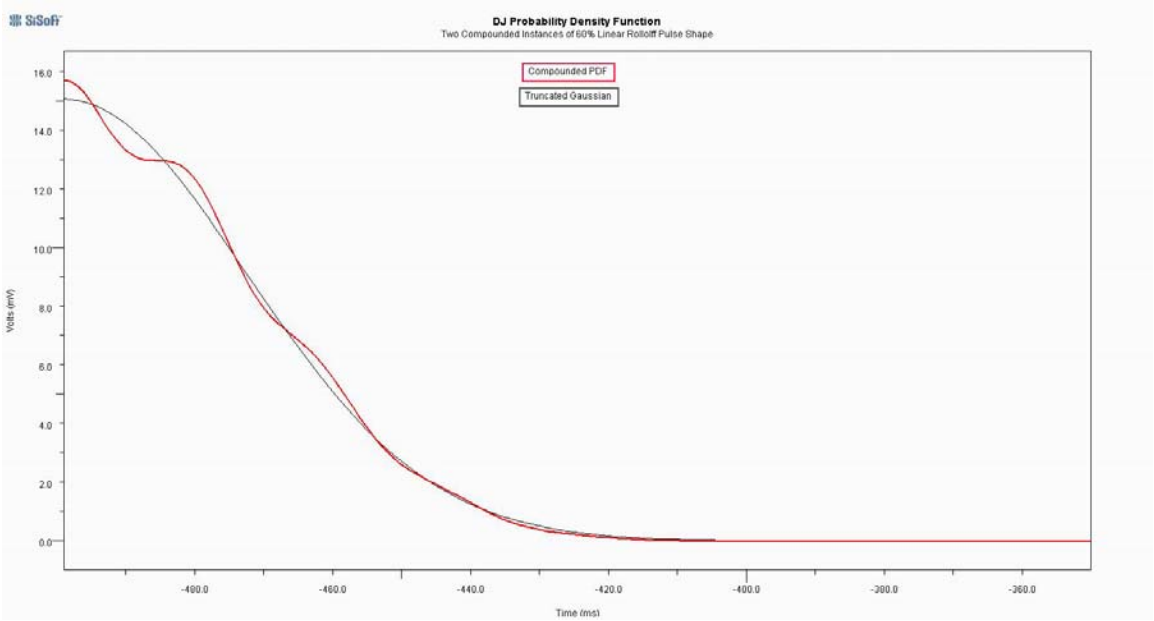

Figure 8: PDF for two instances of the DJ process, together with the corresponding truncated Gaussian

Figure 9 shows the same data as Figure 8, only with a logarithmic vertical scale.

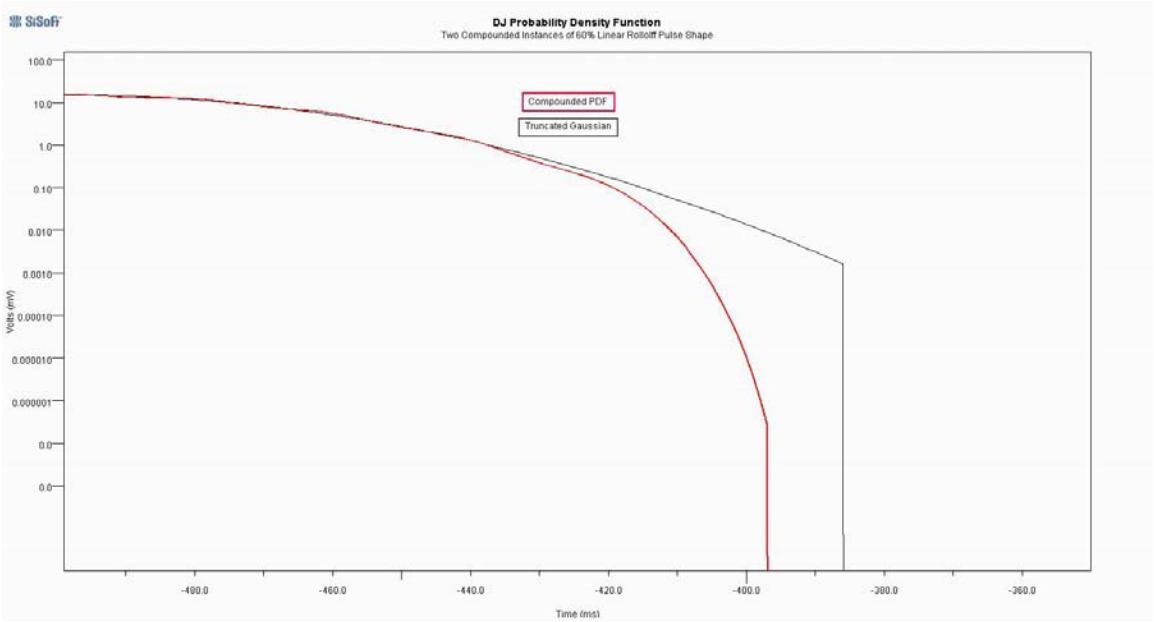

Figure 9: Log plot of PDF for two instances of the DJ process, together with the corresponding truncated Gaussian

It should be noted in Figure 9 that while the peak deviation of the actual distribution should have extended to the same point where the Gaussian was truncated, it appears that the convolved PDF fell off too rapidly to be calculated accurately by the fast Fourier transform method that was used to perform the calculation. Thus, aside from providing a

conservative estimate of the peak deviation, the truncated Gaussian appears to be a useful fit to the data which was obtained with minimal effort.

6.0 Crosstalk

As mentioned in Section 1, crosstalk can be considered to be a form of DJ; and as was the case with intersymbol interference, it would be useful to know what the PDF of the DJ due to crosstalk is. Since crosstalk is assumed to be small compared to the desired signal, the DJ due to crosstalk can be approximated by dividing the amplitude of the crosstalk by the slew rate of the desired signal. Therefore, for crosstalk what is really needed is the amplitude PDF. This amplitude PDF can also be used directly in either a convolution engine or semi-analytical bit error rate estimate.

A distinction must also be made between mesochronous crosstalk (exactly the same data rate as the victim, but arbitrary phase) and plesiochronous crosstalk (not quite the same data rate as the victim). For mesochronous crosstalk, one must obtain the amplitude PDF of the crosstalk as a function of timing relative to the desired signal; whereas with plesiochronous crosstalk, it will suffice to average the amplitude PDF for all times. We will present both results in this section for the 60% linear rolloff response.

One of the primary mechanisms for crosstalk coupling in high speed serial links is the coupling between parallel conductors. As explained in [7], these parallel conductors form a microwave directional coupler. The center frequency of this coupler is

$$f_0 = \frac{1}{\sqrt{\varepsilon_r}} \frac{c}{4l}$$

where l is the length of the coupling section, ε_r is the relative dielectric constant, and c is the speed of light in free space.

As a directional coupler, the coupling section also has a characteristic impedance which is determined by the dielectric constant, the conductor geometries and the geometry and spacing of the ground path. If this characteristic impedance were nearly equal to the characteristic impedance of the surrounding system, then there would be near end crosstalk coupling but very little far end crosstalk coupling. This is seldom the case, however. Usually, the characteristic impedance of the coupling section (as a microwave directional coupler) is significantly lower than that of the surrounding system, resulting in far end crosstalk caused by reflections internal to the coupler.

For a coupler with relatively weak coupling, the near end coupling impulse response is the sum of two impulses: one as the signal enters the coupling section and another of opposite sign as the signal leaves the coupling section. This can be determined by following the derivation given in pages 802-5 of [7]. The equation is

$$h(t) = \frac{k}{2}\left(\delta(t) - \delta\left(t - 2\sqrt{\varepsilon_r}\frac{l}{c}\right)\right)$$

where *k* is the maximum coupling coefficient.

The far end crosstalk coupling has a similar form except that it is delayed by an additional pass through the coupling section and multiplied by the reflection coefficient created by the difference in characteristic impedance between the coupling section and the surrounding system.

The calculations presented here assume that there is only a single coupling section. In practice, this is seldom if ever the case; however, it is often the case that there are one or two dominant coupling sections combined with numerous smaller contributors.

The calculations performed here assume a coupling section length of 0.15UI, or 4.4mm in FR4 at 5Gb/s, and a coupling coefficient *k* of 0.14. These values would be typical for a pair of closely spaced vias in a printed circuit board.

For the 60% linear rolloff response, the coupled crosstalk eye is shown in Figure 10.

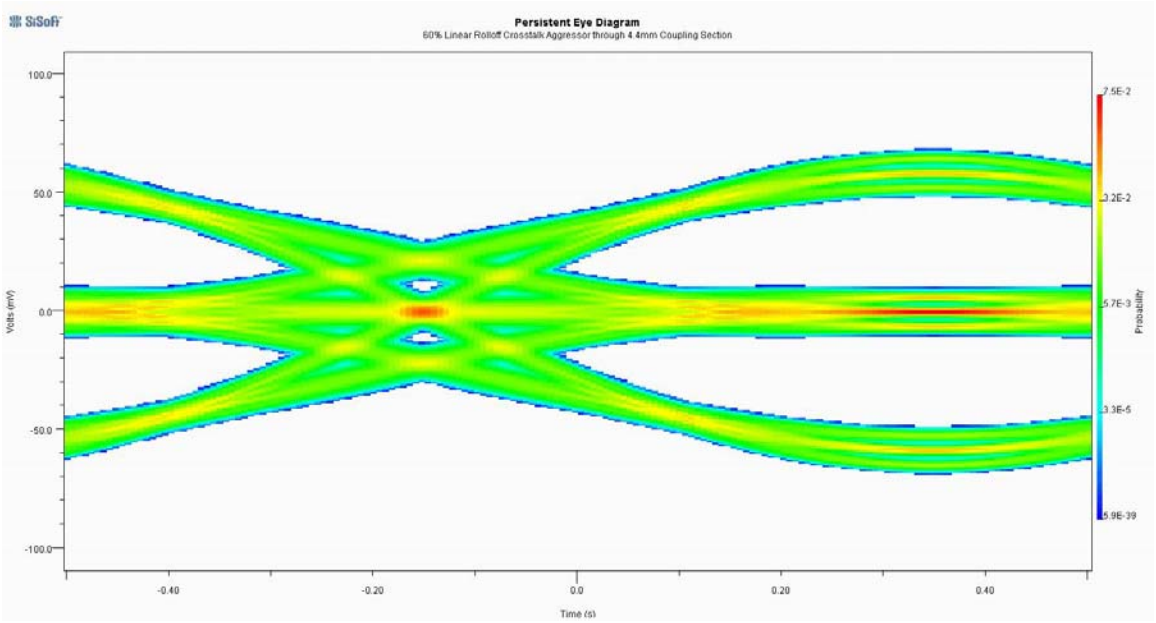

Figure 10: Crosstalk coupled eye for 60% linear rolloff response

The edges of the eye in Figure 10 are quite well defined, suggesting that for a single mesochronous aggressor, the amplitude PDF must definitely be incorporated into the DJ or bit error rate calculation explicitly, and should not be approximated by a Gaussian function. It should also be noted that similar responses have been measured in real systems, although the results were not quite as hard-edged as those shown in Figure 10.

Figure 11 shows the amplitude PDF for a plesiochronous aggressor. This curve was calculated by averaging together all of the amplitude PDFs in Figure 10. Figure 11 also shows the Gaussian which has the same mean and standard deviation as the amplitude PDF.

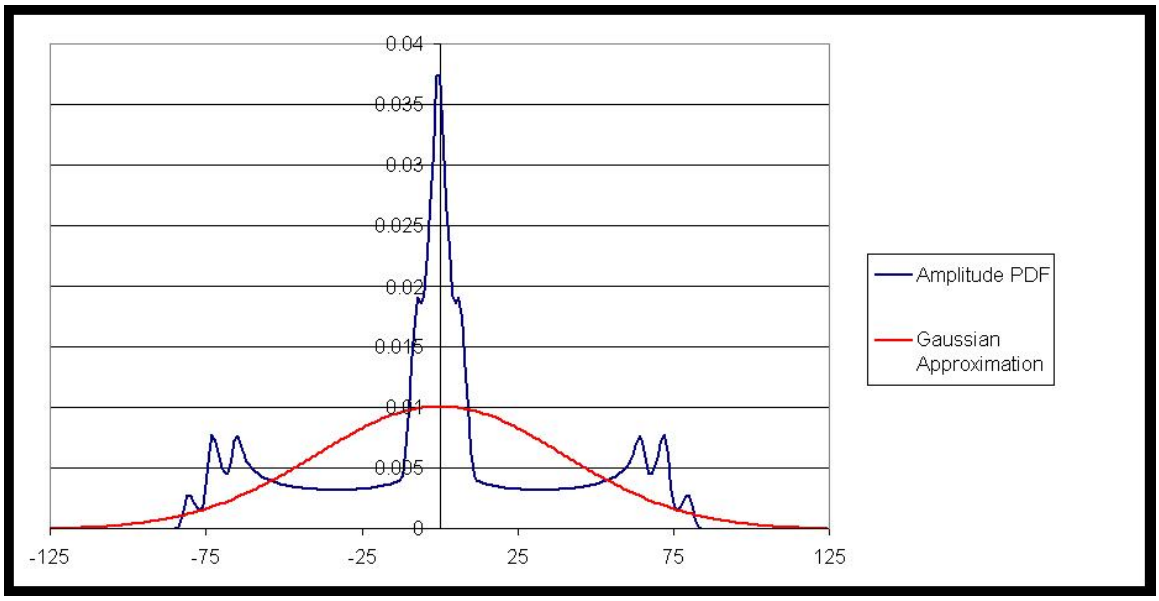

Figure 11: Amplitude PDF for a plesiochronous 60% linear rolloff aggressor

Figure 11 demonstrates that even for a plesiochronous crosstalk aggressor, the Gaussian approximation is not a very good one. In Figure 11, the amplitude PDF does not extend more than two standard deviations to either side of the mean.

Suppose one were willing to combine independent crosstalk aggressors with essentially the same amplitude PDF until the combined PDF approximated a Gaussian down to a probability of 10^{-12}. That means that the peak deviation of the amplitude PDF would have to occur more than seven standard deviations from the mean. Considering that the peak deviation increases linearly with the number of independent terms while the standard deviation increases as the square root of the number of terms, one would have to have 12 crosstalk aggressors with an amplitude PDF similar to that in Figure 11 to get the desired approximation to a Gaussian. This may occur in some applications, but will certainly not always be the case.

7.0 Conclusions

This paper has presented a family of pulse responses that are at least a first order approximation to achievable system responses, and yet can be calculated from closed form equations. Evaluation of intersymbol interference and crosstalk for these pulse responses indicates that DJ distributions truly do have relatively hard edges, but those edges occur several standard deviations from the mean. Thus it is no more reasonable to approximate DJ as uniformly distributed than it is to approximate it as a Gaussian process. This paper has also proposed the use of a truncated Gaussian as an approximation which reflects the general nature of the process while remaining reasonably simple to calculate.

Acknowledgement

This study was motivated by a lively discussion with Al Neves, Ransom Stephens, and Scott McMorrow at DesignCon2007.

References

[1] Bryan Casper, Matthew Haycock and Randy Mooney, “An accurate and efficient analysis method for multi-Gb/s chip to chip signaling schemes”, VLSI Digest of Technical Papers, June 13, 2002, pages 54-7.

[2] Members of the Technical Staff, Bell Laboratories, Transmission Systems for Communications, Bell Laboratories, Inc., Fifth Edition, 1982, pgs. 716-21.
(The Bell Labs "Blue Book")

[3] Djordjević, Biljić, Likar-Smiljanić, and Sarkar, “Wideband Frequency-Domain Characterization of FR-4 and Time-Domain Causality”, IEEE Transactions on Electromagnetic Compatibility, Vol. 43, No. 4, November 2001.

[4] Ramo, Whinnery and Van Duzer, *Fields and Waves in Communication Electronics*, Section 4.5, pages 182-6, John Wiley and Sons, Inc., copyright 1994.

[5] Steinberger, Westerhoff, and White, “Demonstration of SerDes Modeling using the Algorithmic Model Interface (AMI) Standard”, DesignCon 2008 Proceedings, February 2008.

[6] Anthony Sanders, Mike Resso, John D’Ambrosia, “Channel Compliance Testing Utilizing Novel Statistical Eye Methodology”, DesignCon 2004 Proceedings.

[7] Matthei, Young and Jones, *Microwave Filters, Impedance-Matching Networks, and Coupling Structures*, Chapter 13, pages 775-80 and 804-9, McGraw-Hill, copyright 1964.